3. GENERAL PROBLEM SETUP

3.1 Dual Input Describing Function Method

In order to analyze the pilot-aircraft system it is necessary to obtain a model of this system. The use of describing functions offers a good means to analyze multiple nonlinearities. This method allows the linear and nonlinear parts of the system to be separated.[14-19]

Nonlinear portions of the system are defined by a gain, N, who's value is a function of input. This kind of quasi-linearization is called a describing function. Consider Figure 3.1.1, which depicts the block diagram form of a nonlinear describing function element with input, y(t) and output, u(t).

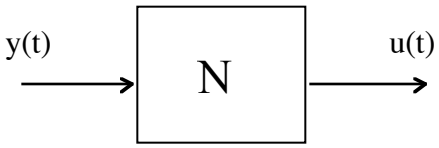

Figure 3.1.1 Block Diagram of Symmetric Saturation Element

Here y(t) will be defined such that it contains an oscillatory and offset part since, ultimately, a solution containing an oscillatory and constant part is desired.

$$y(t) = A\sin(\omega t) + B \qquad (3.1.1)$$

Let us now consider a nonlinear element defined by symmetric saturation with limits of $\pm d$. The input to this signal limiter will be y(t), and the actual limited signal will be piecewise defined as n(t) (Figure 3.1.2).

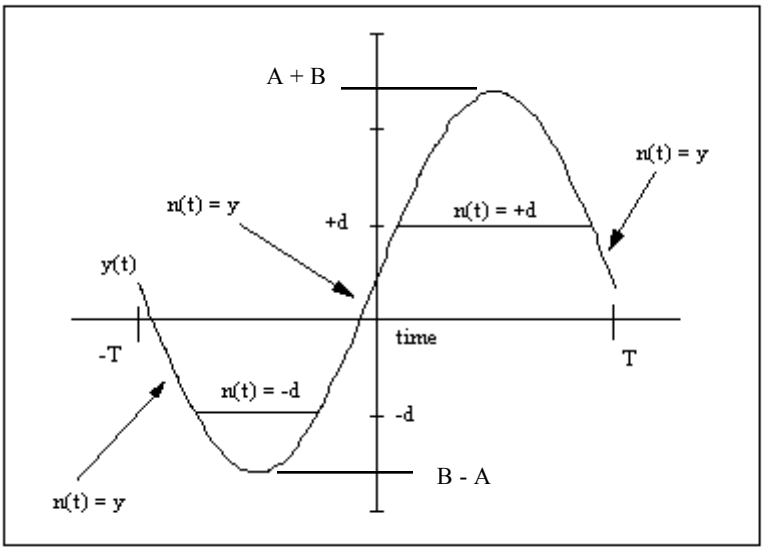

Figure 3.1.2 Symmetric Limiting of Offset Sinusoidal Function

Figure 3.1.2 shows the sinusoidal input, y(t) and the limited signal, n(t). Note that n(t) = y(t) except for points in which |y(t)| exceeds |d|. When this limiting occurs n(t) is set to the limiting value of positive or negative d.

The output signal, u(t), is set equal to the piecewise defined function, n(t), and can be described by a Fourier series expansion such as

$$u(t) = b_0 + a_1\sin\omega t + b_1\cos\omega t + a_2\sin 2\omega t + b_2\cos 2\omega t + \ldots \qquad (3.1.2)$$

where the coefficients are given by

$$a_k = \frac{1}{T}\int_{-T}^{T}\sin(k\omega t)n(t)dt \qquad (3.1.3)$$

$$b_k = \frac{1}{T}\int_{-T}^{T}\cos(k\omega t)n(t)dt \qquad (3.1.4)$$

$$b_0 = \frac{1}{2T}\int_{-T}^{T} n(t)dt \qquad (3.1.5)$$

for k = 1,2,3,4,5,..., ∞ and T is the fundamental period.

Upon integration of these terms, it is discovered that the coefficients are independent of frequency of oscillation, ω, and have the following characteristics:

$a_k = 0, \quad k = 2,4,6,\ldots$

$b_k = 0, \quad k = 1,2,3,\ldots$

leaving

$$u(t) = b_0 + a_1 \sin\omega t + a_3 \sin 3\omega t + \ldots \qquad (3.1.6)$$

Here, the output the signal, u(t), is identical to the actual limited signal, n(t). Several assumptions are made in order to make the sine series describe the nonlinear element behavior. We know that the frequency of interest is ω, the first harmonic. The next frequency that appears is 3ω, and we will assume that this frequency as well as all other harmonics are attenuated by the linear dynamics of the system. This assumption allows us to truncate equation 3.1.6 to this first harmonic with the inclusion of the offset as shown in equation 3.1.7.

$$u(t) = b_0 + a_1 \sin\omega t \qquad (3.1.7)$$

Now, the output signal, u(t), approximates the actual limited signal, n(t).

Recalling Figure 3.1.1, it can be seen that it is necessary to solve for N such that

$$u = N(y)y \qquad (3.1.8)$$

Therefore we will separate the oscillatory and constant portion of the nonlinear element as follows:

$$N_A A = a_1 \tag{3.1.9}$$

$$N_B B = b_0 \tag{3.1.10}$$

which, from equations 3.1.7, allows

$$u(t) = N_A A\sin(\omega t) + N_B B \tag{3.1.11}$$

Rearranging the terms of 3.1.9 and 3.1.10 allows us to solve for N_A and N_B.

$$N_A = a_1/A \tag{3.1.12}$$

$$N_B = b_0/B \tag{3.1.13}$$

N_A and N_B are each dependent upon both A and B because a_1 and b_0 both depend on A and B. For a symmetric limiter, N_A and N_B are defined as follows:[15]

$$N_A = \frac{1}{2}\left[f\left(\frac{d+B}{A}\right) + f\left(\frac{d-B}{A}\right)\right] \tag{3.1.14}$$

$$N_B = \frac{A}{2B}\left[g\left(\frac{d+B}{A}\right) - g\left(\frac{d-B}{A}\right)\right] \tag{3.1.15}$$

where,

$$f(\gamma) = \begin{cases} -1 & \gamma < -1 \\ \frac{2}{\pi}\left(\sin^{-1}(\gamma) + \gamma\sqrt{1-\gamma^2}\right) & |\gamma| \le 1 \\ 1 & \gamma > 1 \end{cases} \tag{3.1.16}$$

$$g(\gamma) = \begin{cases} \frac{2}{\pi}\left(\gamma \sin^{-1}(\gamma) + \sqrt{1-\gamma^2}\right) & |\gamma| \le 1 \\ |\gamma| & |\gamma| > 1 \end{cases} \qquad (3.1.17)$$

The element described by equations 3.1.14 - 3.1.17 applies to symmetric limiters with an offset sinusoidal input. The resulting output given by this element is in the form of an offset sinusoid which is actually the first harmonic of the actual limited signal.[14-19]

3.2 DIDF Applied to Asymmetric Limit

Saturation elements are very common nonlinearities, but often they are not symmetric. Consider an asymmetric saturation element (Figure 3.2.1).

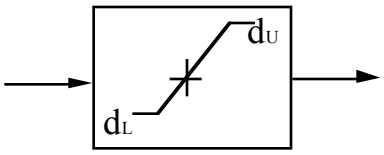

Figure 3.2.1 Asymmetric Saturation

The upper signal limit is d_U and the lower limit is d_L. It is necessary to obtain a method to account for this asymmetry in order to accurately model this limiting characteristic.

It is possible to treat such asymmetric saturation through the use of the nonlinear element described in section 3.1. The process of applying this nonlinear element to asymmetric saturation begins with the following definition:

$$d_U = d + c \qquad (3.2.1)$$

$$d_L = -(d - c) \qquad (3.2.2)$$

where ± d is still the range of motion permitted without saturation. The variable, c, is the center of this range. The application of this method is demonstrated in the following block diagram (Figure 3.2.2)

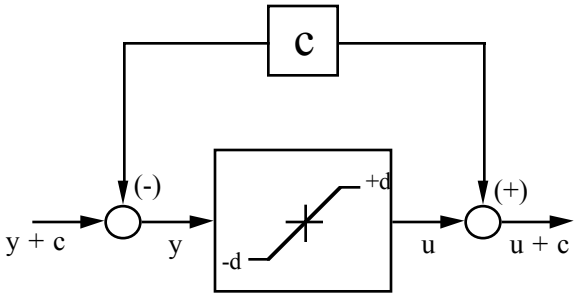

Figure 3.2.2 Block Diagram of Asymmetric Limiter

It can be seen from figure 3.2.2 that y(t) + c is now the input to the asymmetric limit and u(t) + c is the output of the asymmetric limit. We will now define

$$\hat{u}(t) = u(t) + c \qquad (3.2.3)$$

$$\hat{y}(t) = y(t) + c \qquad (3.2.4)$$

which defines the complete input, $\hat{y}$, to output, $\hat{u}$, of the asymmetric limit. It is now possible to use this symmetric saturation DIDF to model asymmetric saturation.

3.3 Definition of Problem Structure

The describing function method requires that the complete system be split into two parts. This system is shown in block diagram form in Figure 3.3.1. One of these parts is purely linear and will be defined as M(s). The other portion of the model is quasi-linear and will be defined by DIDF with input vector, $\hat{y}$, and output vector, $\hat{u}$.

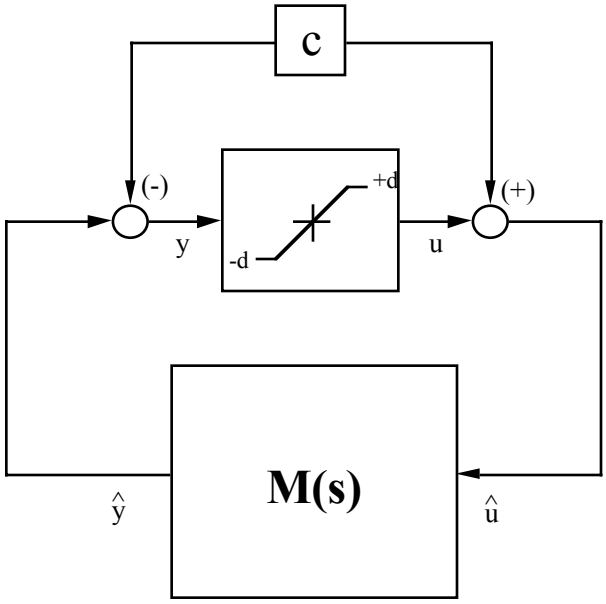

Figure 3.3.1 Block Diagram of Nonlinear System with Asymmetric Saturation

It can be seen that the input vector to M(s) is $\hat{u}$, and the output vector from M(s) is $\hat{y}$. This relationship can be expressed in state-space form as

$$\dot{x} = Fx + G\hat{u} \tag{3.3.1}$$

$$\hat{y} = Hx \tag{3.3.2}$$

Note that both $\hat{y}$ and $\hat{u}$ are vectors with column length equal to the number of nonlinearities present in the system.[19]

Through the use of equations 3.2.3 and 3.2.4, these equations may be rewritten as

$$\dot{x} = Fx + G(u + c) \tag{3.3.3}$$

$$y = Hx - c \tag{3.3.4}$$

where

$$u = N(y)y \tag{3.3.5}$$

and N(y) is a diagonal matrix of symmetric saturation DIDF's. This matrix is square and equal to the number of nonlinearities present in the system.

The desired solution of equations 3.3.3 - 3.4.5 contains both an oscillatory part (limit cycle) and a constant part (mean point of oscillation). Therefore, the solution method is split into an oscillatory and constant portion. The oscillatory part of the system will be denoted by a subscript s and the constant part with a subscript c. The result of applying this procedure to the state equations, 3.3.3 and 3.3.4, is

$$\dot{x} = \dot{x}_s + \dot{x}_c = F(x_s + x_c) + G(u_s + u_c + c) \tag{3.3.6}$$

$$y = y_s + y_c = Hx_s + Hx_c - c \tag{3.3.7}$$

The describing function inputs are given by equation 3.1.1 which may be rewritten as

$$y_s = A\sin(\omega t) \tag{3.3.8}$$

$$y_c = B \tag{3.3.9}$$

and the describing function outputs are given by equation 3.1.11,

$$u_s = N_A A\sin(\omega t) \tag{3.3.10}$$

$$u_c = N_B B \tag{3.3.11}$$

where both N_A and N_B have the same size as N, and A and B are vectors of length equal to the number of nonlinearities present in the system.

Now, the state equations, 3.3.6 and 3.3.7 will be separated by their oscillatory and constant parts.

$$\dot{x}_s = Fx_s + Gu_s \tag{3.3.12}$$

$$y_s = Hx_s \tag{3.3.13}$$

$$\dot{x}_c = Fx_c + G(u_c + c) \tag{3.3.14}$$

$$y_c = Hx_c - c \tag{3.3.15}$$

The solution now depends on obtaining a solution for u_s and u_c in terms of the state variables, x_s and x_c. Combining equations 3.3.8 and 3.3.10 gives

$$u_s = N_A\, y_s \tag{3.3.16}$$

and, similarly, combining equations 3.3.9 and 3.3.11 gives

$$u_c = N_B y_c \tag{3.3.17}$$

With the use of equations 3.3.16 and 3.3.13 it can be shown that

$$u_s = N_A H x_s \tag{3.3.18}$$

$$u_c = N_B H x_c - N_B c \tag{3.3.19}$$

Finally, two equations can be found that govern, separately, the oscillatory and constant parts of the solution. The equation that dictates the oscillatory solution is made by substituting equation 3.3.18 into 3.3.12, which gives

$$\dot{x}_S = (F + GN_A H)x_S \tag{3.3.20}$$

The equation that governs the constant solution is obtained by substituting equation 3.3.19 into 3.3.14 which yields

$$\dot{x}_c = (F + GN_B H)x_c + G(I - N_B)c \tag{3.3.21}$$

The specific solution involving x_s is obtained by combining equations 3.3.8 and 3.3.13 to give

$$A = |Hx_s| \tag{3.3.22}$$

and the specific solution involving x_c is obtained by combining equations 3.3.9 and 3.3.15 which yields

$$B = Hx_c - c \tag{3.3.23}$$

3.4 Solution Method for Multiple Asymmetric Saturation Elements

Now that two equations have been developed that dictate the solution to the nonlinear system, we can investigate a method of solution. Although it is true that equation 3.3.20 governs the oscillatory solution and equation 3.3.21 governs the constant solution, it is important to remember that these equations are coupled. Recall that both N_A and N_B depend on each A and B. This implies that N_A and N_B are related and therefore the oscillatory solution and the constant solution are related as well. Since the oscillatory and constant motion are interdependent a solution method must be based on the simultaneous solution of both equations 3.3.20 and 3.3.21.

The oscillatory portion of the solution is determined by the existence of a limit cycle. This limit cycle may be found through the use of equation 3.3.20, which is actually an eigenvalue problem described by

$$0 = [F+GN_AH - I\lambda]x_s \tag{3.4.1}$$

In the case of limit cycle existence, an eigenvalue pair with a zero real part will be present. In this case, the eigenvalue is $\lambda = \pm j\omega$ where ω is the frequency of oscillation. The solution is then given by

$$x_s(t) = \varphi\hat{x}_s e^{\pm j\omega t} \tag{3.4.2}$$

where φ is a scalar constant and $\hat{x}_s$ is the norm-one eigenvector corresponding to the given eigenvalue. Note that this is an undamped oscillatory mode of frequency, ω.[14-19]

There are a number of algorithms that have been developed to solve such a problem. Generally, an iterative method is employed to solve this nonlinear problem. A generalized Newton-Raphson method is a popular solution scheme as well as homotopy algorithm methods.[6,12,20-22] It is also possible to use graphical methods to solve these problems.[23] Recently, Anderson proposed a gradient based minimization method that searches over the phasor vector $x_s=x_{sR} + jx_{sI}$.[19] Classically, these algorithms are based on single variable functions, $N_A(A)$. Since the system we are concerned with has a two variable dependence, $N_A(A,B)$ and $N_B(A,B)$, a method of solution must be modified to account for this fact.

It is possible to use a number of different techniques to solve the constant part of the solution in addition to the oscillatory part. However, it is desirable to find a method of solution that can be applied to a system with one or more nonlinearities. Therefore a general method of solution will be described.

First, the number of nonlinearities will be defined as n, and the number of state variables will be defined as m. The solution employed will rely on solving for the n x1 column vectors, A and B, using an iterative method. Since there are 2n variables, A_{nx1} and B_{nx1}, it will be necessary to establish 2n equations which govern these variables. One set of the 2n equations will involve a function which searches for zero real parts of eigenvalue pairs as defined by 3.4.1. This scalar function can be defined as

$$0 = \min_i \left| \mathrm{Re}[\lambda_i (F + G N_A H)] \right| \qquad 3.4.3$$

The oscillatory part of the solution, N_A, can be obtained through the use of equation 3.4.3. However, N_A has a dimension of n x n. Additional constraints must be placed upon equation 3.4.3 in order to guarantee that values of N_A are found that represent an actual limit cycle. It is possible to have many different combinations of values in the elements of N_A that yield purely imaginary eigenvalue pairs. However, not all of these are limit cycle solutions. A method to determine which solutions are valid limit cycle solutions must be developed.

A valid limit cycle solution may be determined by analyzing the vector A, which governs the amplitudes of oscillation. Recall that the vector A has length n and can be defined as

$$A = \begin{bmatrix} A_1 \\ A_2 \\ \vdots \\ A_n \end{bmatrix} \qquad (3.4.4)$$

Similarly, the matrix H, which has dimension n x m, will be partitioned by rows as

$$H = \begin{bmatrix} H_1 \\ H_2 \\ \vdots \\ H_n \end{bmatrix} \qquad (3.4.5)$$

Now, recalling equation 3.3.22 and incorporating equation 3.4.2, it can be shown that

$$\begin{bmatrix} A_1 \\ A_2 \\ \vdots \\ A_n \end{bmatrix} = \varphi \left| \begin{bmatrix} H_1 \\ H_2 \\ \vdots \\ H_n \end{bmatrix} \hat{x}_s \right| \tag{3.4.6}$$

Finally, solving for φ gives

$$\varphi = \frac{A_1}{|H_1 \hat{x}_s|} = \frac{A_2}{|H_2 \hat{x}_s|} = \ldots = \frac{A_n}{|H_n \hat{x}_s|} \tag{3.4.7}$$

It is necessary that both equations 3.4.7 and 3.4.3 be satisfied for a limit cycle solution to exist.

It is now possible to write an equation which is a function of both A and B and gives a solution for N_A. First, the constant, φ, will be rewritten as

$$\varphi_1 = \frac{A_1}{|H_1 \hat{x}_s|}, \varphi_2 = \frac{A_2}{|H_2 \hat{x}_s|}, \ldots, \varphi_n = \frac{A_n}{|H_n \hat{x}_s|} \tag{3.4.8}$$

where, if a limit cycle oscillation is found,

$$\varphi = \varphi_1 = \varphi_2 = \ldots = \varphi_n \tag{3.4.9}$$

Through the use of equations 3.4.3 and 3.4.8 the following positive definite function can be defined:

$$0 = \min_i \left| \mathrm{Re}[\lambda_i (F + G N_A H)] \right| + |\varphi_n - \varphi_1| + |\varphi_n - \varphi_2| + \ldots + |\varphi_n - \varphi_{n-1}| \tag{3.4.10}$$

{ n equations , 2n unknowns ($A_1, A_2, \ldots, A_n$ and $B_1, B_2, \ldots, B_n$) }

This solution applies to any system with multiple describing function elements. A system containing only single input describing function elements could be solved through the use of equation 3.4.10 alone. However, the solution to a system with

DIDF's requires that another function be defined in order to solve for limit cycle solutions of the system.

The second function involves a solution for N_B. It is necessary that $\dot{x}_c = [0]_{nx1}$ for a constant solution to exist. This fact can be applied to equation 3.3.21 to give

$$[0]_{nx1} = (F + GN_BH)x_c + G(I - N_B)c \qquad (3.4.11)$$

which can be rewritten as

$$x_c = -(F+GN_BH)^{-1}G(I-N_B)c \qquad (3.4.12)$$

where I has a dimension of n x n and c has a dimension of n x 1.

Equation 3.4.12 can be combined with equation 3.3.23 to give

$$B = -H(F+GN_BH)^{-1}G(I-N_B)c - c \qquad (3.4.13)$$

which can be rearranged to give

$$[0]_{nx1} = B + c + H(F+GN_BH)^{-1}G(I-N_B)c \qquad (3.4.14)$$

{ n equations, 2n unknowns, (A_1, A_2,…, A_n and B_1, B_2,…, B_n) }

A limit cycle solution is found when equation 3.4.14 and equation 3.4.10 are both satisfied.

An equation may now be written that determines the limit cycle solutions of a system containing multiple DIDF's. The limit cycle solution will be found using equations 3.4.10 and 3.4.14 to write a cost function that can be minimized by a gradient based minimization routine.

First, equation 3.4.14 can be set equal to a column vector, ψ,

$$\begin{Bmatrix} \psi_1 \\ \psi_2 \\ \vdots \\ \psi_n \end{Bmatrix} = B + c + H(F + GN_B H)^{-1} G(I - N_B)c \qquad (3.4.15)$$

Through the use of equations 3.4.10 and 3.4.15 a positive definite cost function can be written as follows:

$$J = \min_i \left| \mathrm{Re}[\lambda_i (F + GN_A H)] \right| + |\varphi_n - \varphi_1| + |\varphi_n - \varphi_2| + \ldots + |\varphi_n - \varphi_{n-1}|$$

$$+ |\psi_1| + |\psi_2| + \ldots + |\psi_n| \qquad (3.4.16)$$

{ 2n equations, 2n unknowns (A_1, A_2,…, A_n and B_1, B_2,…, B_n) }

where J is minimized and ideally should be zero. The values of A and B and the frequency of oscillation, ω, will be given by equation 3.4.16.

The values of A and B can be used to predict amplitudes and mean points of oscillation as they apply to the state variables. Magnitudes of oscillation can be determined through the use of equation 3.4.2, which can be rearranged as

$$\left| x_s \right| = \varphi \left| \hat{x}_s \right| \qquad (3.4.17)$$

and the m-dimensional mean point of oscillation can be calculated using equation 3.4.12.

Implementation of this method requires that initial guesses be made for the variables A and B. These guesses can be made by guessing the amount of limiting in each of the saturation elements ($N_{A(1,1)}$,$N_{A(2,2)}$,...,$N_{A(n,n)}$). Initial values of A and B are determined by the following relations:

$$A_i = \frac{d_i}{N_{A(i,\,i)}} \quad i = 1, 2, \ldots, n \qquad (3.4.18)$$

$$B_i = \frac{-c_i}{N_{A(i,i)}} \quad i = 1, 2, ..., n \tag{3.4.19}$$

where

$$B = \begin{bmatrix} B_1 \\ B_2 \\ \vdots \\ B_n \end{bmatrix} \tag{3.4.20}$$

$$d = \begin{bmatrix} d_1 \\ d_2 \\ \vdots \\ d_n \end{bmatrix} \tag{3.4.21}$$

and

$$c = \begin{bmatrix} c_1 \\ c_2 \\ \vdots \\ c_n \end{bmatrix} \tag{3.4.22}$$

Note that all elements of N_A must be in the range of (0,1], which gives a good bound on the possible initial guesses of A and B. Also, it may be necessary to scale each component of equation 3.4.16 in order to easily converge upon a solution.

3.5 Validation of DIDF Method / Example

As stated previously, The describing function method is an approximation to the exact solution. Therefore, it is necessary to determine the accuracy that can be expected from the use of DIDF to represent asymmetric saturation. Predicted values obtained through the use of the methods in section 3.4 must be compared to that of simulated solutions. Simulated solutions can be obtained through the use of a numerical integration scheme.

Consider the following 3rd order system with one asymmetric limit.[27]

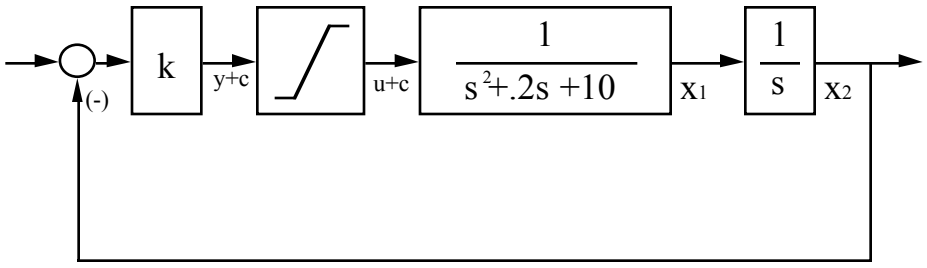

Figure 3.5.1 Block Diagram of Dynamic System with One Asymmetric Limit

Here, the gain, k, multiplies the state variable, x_2. Notice that the input and output of the saturation element are $y + c = \hat{y}$ and $u + c = \hat{u}$, respectively. The constant, c, is the offset of saturation and d is the amplitude of the limit. Recall the upper limit is (d + c) and the lower limit is -(d - c).

The block diagram in Figure 3.5.1 may be written in state space form as

$$\begin{Bmatrix} \ddot{x}_1 \\ \dot{x}_1 \\ \dot{x}_2 \end{Bmatrix} = \begin{bmatrix} -0.2 & -10 & 0 \\ 1 & 0 & 0 \\ 0 & 1 & 0 \end{bmatrix} \begin{Bmatrix} \dot{x}_1 \\ x_1 \\ x_2 \end{Bmatrix} + \begin{bmatrix} 1 \\ 0 \\ 0 \end{bmatrix} \hat{u} \tag{3.5.1}$$

$$\hat{y} = \begin{bmatrix} 0 & 0 & -k \end{bmatrix} \begin{Bmatrix} \dot{x}_1 \\ x_1 \\ x_2 \end{Bmatrix} \tag{3.5.2}$$

Limit cycle solutions for this system can be found through the use of equation 3.4.16. Since there is only one asymmetric saturation element in this system, equation 3.4.16 reduces to

$$J = \min_i \left| \mathrm{Re}[\lambda_i (F + GN_A H)] \right| + |\psi| \tag{3.5.3}$$

where

$$\psi = B + c + H(F+GN_BH)^{-1}G(1-N_B)c \qquad (3.5.4)$$

Equation 3.5.3 is minimized by a gradient based minimization algorithm. This algorithm is implemented by use of the MATLAB® Optimization Toolbox function, *fminu*.

A variety of gains, k, are used to induce varied amounts of limiting through the asymmetric saturation element. In this example, the asymmetric saturation element is defined to have an upper limit of $d_U = 1.5$ and a lower limit of $d_L = -0.5$. Recall from equations 3.2.1 and 3.2.2 that these limits corresponds to a value of d = 1.0 and c = 0.5.

An analysis of the linearized (unsaturated) system reveals that instability occurs at a value of k greater than 2. Therefore, simulations of the system will be performed for values of k greater than 2. Non-zero initial conditions must be used in order to obtain deviation from a steady state. The initial conditions will be set to

$$\begin{Bmatrix} \dot{x}_1 \\ x_1 \\ x_2 \end{Bmatrix} = \begin{Bmatrix} 0 \\ 0 \\ 1 \end{Bmatrix} \qquad (3.5.1)$$

Unstable motion that is created for these values of k is limited by the asymmetric saturation element. The resulting motion is a limit cycle. Variations of k above k greater than 2 causes the nature of the limit cycle to change. Limit cycles are simulated through the use of the 5th order Runge-Kutta numerical integration method.[24-26] A comparison of simulated and predicted solutions for a variety of gains, k, is presented in Table 3.5.1

Table 3.5.1 Simulated and Predicted Solutions for the Example

	SIMULATED					PREDICTED								
k	ω	$\lvert X_{s1}\rvert$	$\lvert X_{s2}\rvert$	X_{c1}	X_{c2}	ω	$\lvert X_{s1}\rvert$	$\lvert X_{s2}\rvert$	X_{c1}	X_{c2}	A	B	N_A	N_B
3	3.22	1.14	0.361	0.002	0.073	3.16	1.14	0.361	0	0.071	1.08	-0.71	0.67	0.70
4	3.22	1.24	0.393	0.008	0.128	3.16	1.24	0.393	0	0.125	1.57	-1.00	0.50	0.50
5	3.22	1.32	0.416	0.009	0.168	3.16	1.30	0.411	0	0.165	2.05	-1.32	0.40	0.38
6	3.22	1.34	0.425	0.009	0.198	3.16	1.33	0.423	0	0.195	2.54	-1.67	0.33	0.30
7	3.22	1.36	0.432	0.009	0.223	3.16	1.36	0.431	0	0.219	3.02	-2.04	0.29	0.25
8	3.22	1.38	0.437	0.009	0.240	3.16	1.39	0.437	0	0.237	3.50	-2.39	0.25	0.20

Table 3.5.1 presents predicted results obtained from the methods of Section 3.4 and simulated results obtained through the use of a 5th order Runge-Kutta numerical integration scheme. Numerical integration was performed with a step size of h = 0.01 sec. The gain, k, is shown in the first column and ranges from 3 to 8. Oscillation frequency in rad/s is shown in the first column for both SIMULATED and PREDICTED data. Amplitudes of oscillation for state variables x_1 and x_2 are presented in the next columns, followed by the mean points of oscillation, x_{c1} and x_{c2}. The next two columns show the estimated values of input to the saturation element , and the last two columns show the amount of saturation present in the element.

It can be seen from Table 3.5.1 that the amount of limiting indicated by the size of u_s, N_A, increases steadily as gain, k, is increased. The amount of offset limiting also increases at about the same rate.

It can also be seen from Table 3.5.4 that the predicted frequency is slightly lower than that of the simulated frequency. Still, these results are quite good, and the accuracy of the predicted results is more than satisfactory.

The magnitudes and offsets of oscillation are of great importance to the nature of any limit cycle. The amplitudes of oscillation give information as to how dramatic the limit cycle behavior of the nonlinear system is, and the offsets of oscillation indicate how much asymmetric motion occurs due to the asymmetric limits.

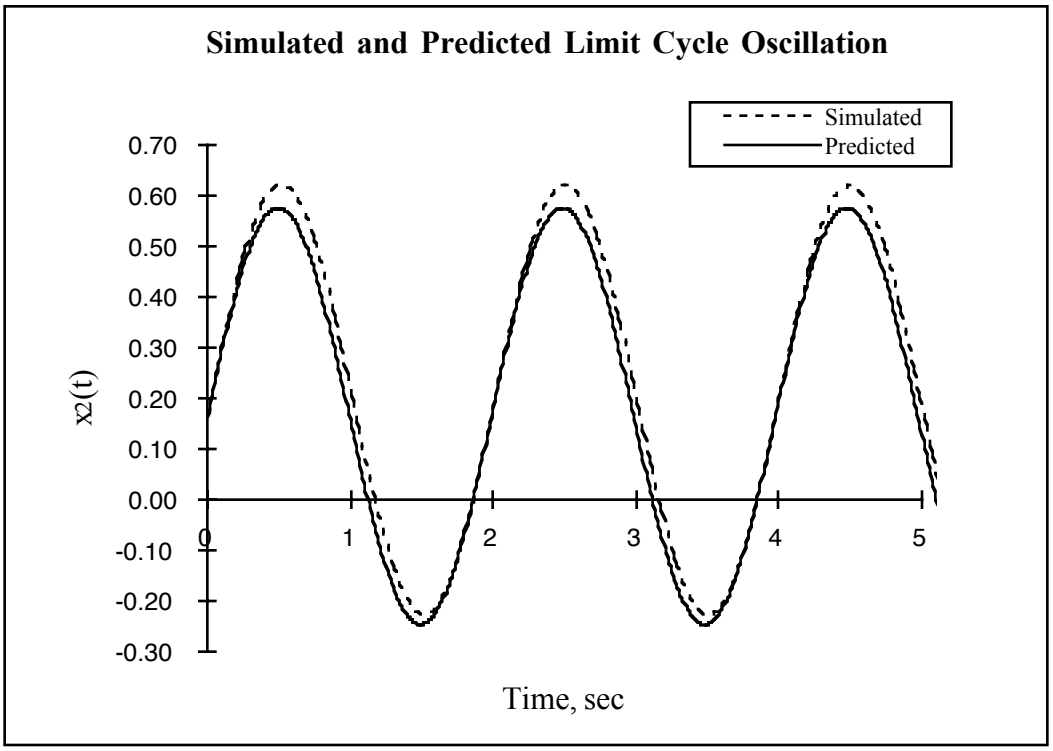

Figure 3.5.2 Time history of Simulated and Predicted Limit Cycle Solution for State Variable x_2 for Gain, k=6

Figure 3.5.2 is a representation of the oscillation that occurs in state variable, x_2, for a gain of k = 6. It can be seen that the Simulated and Predicted limit cycle oscillations match quite well. Both show an offset of oscillation of about 0.2, and both have an

amplitude of about 0.4. These results are very encouraging. The degree of accuracy is almost surprising considering the approximation methods used in the DIDF. Predicted amplitudes of oscillation are slightly less than simulated values for gains, k, in the range from 4 to 7. However, these differences are less than 1.5 %.

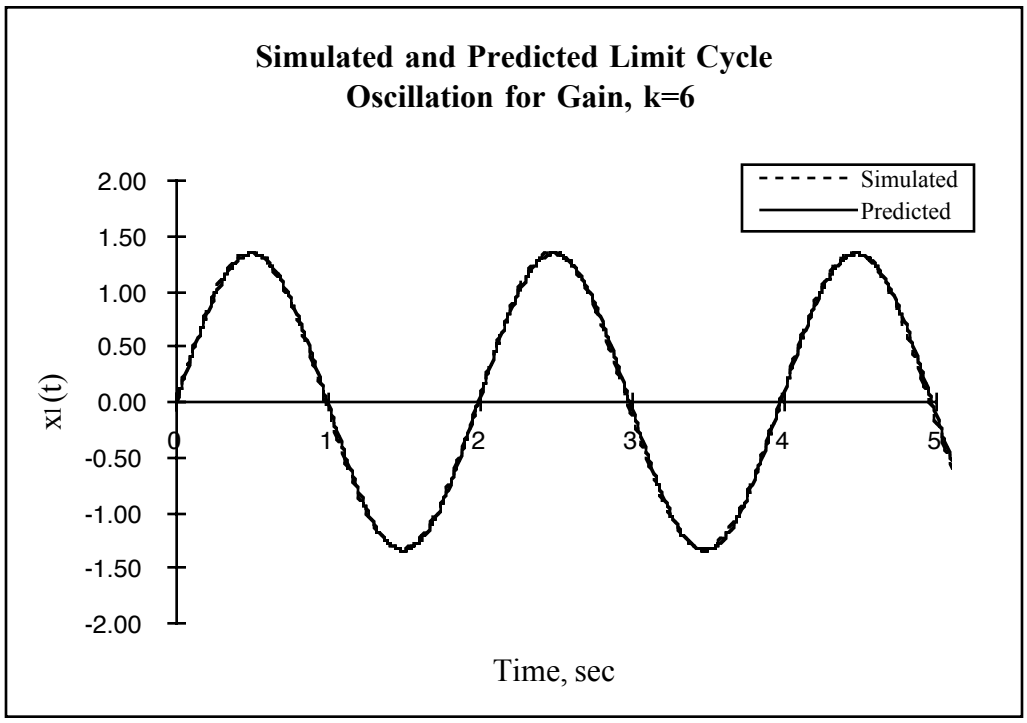

Figure 3.5.3 Time history of Simulated and Predicted Limit Cycle Solution for State Variable x_1 for Gain, k=6

Figure 3.5.3 is a representation of the oscillations that occur in state variable, x_1, for a gain of k = 6. Once again, simulated and predicted limit cycle oscillations are in good agreement. Both simulated and predicted magnitudes of oscillation are about 1.3. However, the simulated mean point of oscillation is about 0.02 while the predicted offset of oscillation is strictly zero.

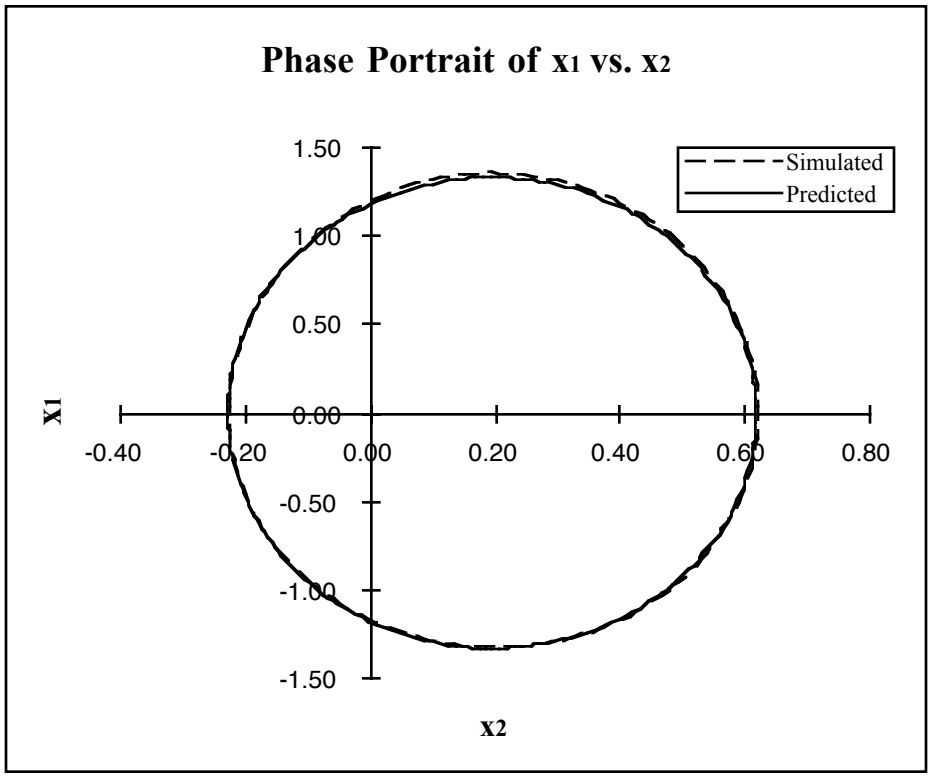

Figure 3.5.4 Phase Portrait of Simulated and Predicted Limit Cycle Solution for Gain, k=6

Figure 3.5.4 shows that the overall elliptic shape of the limit cycle oscillation is predicted very accurately. However, examination of Table 3.5.1 shows that the offset of x_1 is predicted to be zero for all gains, k. Conversely, the simulated offset of x_1 varies with changes in k. An explanation of this phenomenon is necessary.

3.6 Limitations of DIDF Method

It is important to recognize that the describing function method is only an approximate method to calculate limit cycles. Recall that this method uses the fundamental frequency of oscillation to represent the complete motion of the limit cycle. Due to this fact, it is possible that the limit cycle may not be accurately represented by the describing function approach.

The describing function method may give inaccurate predictions if the amount of saturation in the nonlinear elements is very high. This result is due to the fact that a high degree of saturation causes the limited signal to take on the shape of a square wave. The describing function attempts to replace this square wave by a single sinusoid of fundamental frequency. This characteristic will be evident if values of N_A are close to zero. Higher degrees of accuracy can be expected if the values of N_A are close to one, in which case the limited signal will be more like a sinusoid.

Even if saturation levels are high, it is still possible that the describing function method will provide accurate results. As stated previously, the system will attenuate some of the higher harmonics of the limited signal. Depending on the specific system being examined, the attenuation effect can lead to improved accuracy. This example demonstrated good accuracy of the predicted amplitudes of oscillation through a wide variety of gains. This accuracy can be attributed to the fact that the simulated limit cycle oscillations had a predominantly elliptical shape, as shown in Figure 3.5.4.

Recall that the DIDF prediction method uses single sinusoid approximations to represent the actual limit cycle. Therefore, predicted limit cycle oscillations will always have an elliptical shape. Accuracy of predicted solutions is dependent upon the shape of the actual limit cycle. As the shape of the actual limit cycle becomes non-elliptical, the DIDF prediction method will lose accuracy.

The use of DIDF's for predicting mean points of oscillation also has its limitations. Consider the signal of the state variable x_2 during a limit cycle.

$$x_2(t) = x_{s2}\sin(\omega t) + x_{c2} \tag{3.6.1}$$

According to equation 3.5.1, the derivative of the state variable, x_2, is the state variable, x_1, which can be written as

$$\frac{d}{dt}x_2 = x_1 = \omega x_{s2}\cos(\omega t) \tag{3.6.2}$$

Note that x_1 is predicted to have no mean point of oscillation. This fact is a result of the DIDF approximation which represents the limit cycle oscillation as a single sinusoid. It can be seen that all state variables that are the derivative of another state variable are predicted to have a zero mean point of oscillation. This limitation of the DIDF that must be recognized to successfully employ the DIDF method.